HIROSAKI UNIVERSITY

Radiation Emergency Medicine 2015 Vol.4, No.2 45–52

REM
Radiation Emergency Medicine

Note

Comparison between Irradiation Side Sampling Flat-Panel Detector System and Computed Radiography System for Reduction of Radiation Exposure

Kohsei Kudo[1]*, Minoru Osanai[1], Junichi Hirota[1], Tuyosi Abe[2], Mayu Matsuoka[2], Satoshi Naraki[2], Akira Fujimori[2], Yoshihiro Takai[2, 3] and Yoichiro Hosokawa[1]

[1]*Hirosaki University Graduate School of Health Sciences, 66-1 Hon-cho, Hirosaki, Aomori 036-8564, Japan*
[2]*Department of Radiology, Hirosaki University School of Medicine and Hospital, 53 Hon-cho, Hirosaki, Aomori 036-8563, Japan*
[3]*Department of Radiology and Radiation Oncology, Hirosaki University Graduate School of Medicine, 5 Zaifu-cho, Hirosaki, Aomori 036-8562, Japan*

Received 28 February 2015; revised 3 June 2015; accepted 25 June 2015

As digital image equipment for X-ray, computed radiography (CR) systems and flat-panel detector (FPD) systems have become the mainstream. Additionally, newer FPD systems have been developed that offer high-resolution irradiation side sampling (ISS-FPD), and reduction of each patient incident skin dose is expected. Accordingly, we measured image qualities of an ISS-FPD system and a CR system and compared them for the purpose of reducing radiation exposure. In comparing a lying-position X-ray photographing table-integrated ISS-FPD and a CR system, pre-sampled modulation transfer functions (pre-sampled MTFs), normalized noise power spectrums (NNPSs), and detective quantum efficiencies (DQEs) were measured. Furthermore, visual evaluations by the use of image quality figures (IQFs) were carried out by photographing Burger phantoms. As a result, DQEs of the ISS-FPD were higher and suggested the reduction of radiation exposure by approximately 50%. Also, in the visual evaluation, IQFs of the ISS-FPD system were lower than those of the CR system, suggesting that radiation exposure can be reduced. Our results indicate that this method does not evaluate performance of an image receptor as a single unit but can compare reduction of radiation exposure by calculating the DQE even in image equipment with an integrated grid.

Key words: flat-panel detector, computed radiography, reduction of radiation exposure, image quality

1. Introduction

As digital image devices have been developed, the use of computed radiography (CR) systems[1)] in X-ray diagnostics, began in 1983 and flat-panel detector (FPD) systems were used clinically starting in 1998. FPDs with direct conversion systems or indirect conversion systems are now widespread[2)]. Regarding these machines, there have been some reports[3-6)] that focus on the reduction of radiation exposure, and improvement of imaging conditions is expected to continue to further reduce of radiation exposure. In the CR system, laser light is irradiated to an imaging plate (IP) after X-ray irradiation,

*Kohsei Kudo, PhD: Hirosaki University Graduate School of Health Sciences, 66-1 Hon-cho, Hirosaki, Aomori 036-8564, Japan
E-mail: kohsei@hirosaki-u.ac.jp

Table 1. Details of digital imaging systems used in this study

System	ISS-FPD	CR
Product name	CALNEO MT(Bucky table)	FCR9502HQ(Bucky table)
Manufacure	FUJIFILM Corporation	FUJIFILM Corporation
Detector	Scintillator(Gb_2O_2S:Tb)	Storage phosphor [$BaFX:Eu^{2+}$(X=Cl, Br, I)]
Table	Wood	Wood
Attenuation equivalent of table	1.7mmAl less or epual	1.7mmAl less or epual
Grid ratio	10:1(Movig grid)	8:1(Movig grid)
Console	Console Advance(DR-ID 300CL)	CR Console(DR-IR 348/CR-IR346CL)
Pixel size(mm)	0.15	0.1
Bit depth(bits)	12	10

and a reading device in the IP measures generated photostimulable luminescence. In the indirect FPD, light generated by X-ray irradiation of a phosphor-emitting light is measured with a photodiode. Irradiation of laser light is therefore not necessary, and the phosphor is integrated within the measuring component. As an indirect FPD, a penetration side sampling flat-panel device (PSS-FPD) with a photodiode located behind a phosphor was general systems, but a high-resolution irradiation side sampling flat-panel device (ISS-FPD) with a photodiode located in front of the phosphor was recently developed.[7)]

Tanaka *et al*[8)] compared image qualities of an ISS-FPD and conventional CR for the purpose of the reduction of a patient's skin dose in chest radiography and reported that a reduction of radiation exposure by approximately 50% is possible in the case of the ISS-FPD. On the other hand, with regard to devices used for abdominal X-rays, since there is a larger number that have an FPD or an IP integrated within the lying-position X-ray photographing table (Bucky table), the image quality of an image receptor itself cannot necessarily be measured.

For the purpose of reducing radiation exposure, we measured the image qualities of an ISS-FPD system and a CR system with a lying-position, integrated-type X-ray photographing table, from which a grid is difficult to remove and where an image receptor and a moving grid were fitted. In evaluation of image quality, pre-sampled modulation transfer functions (MTFs), normalized noise power spectrums (NNPSs), and detective quantum efficiencies (DQEs) were measured in conformity with the International Electrotechnical Commission (IEC) 62220-1[10)] at radiation qualities of RQA5 and RQA7[9)]. Furthermore, Burger phantoms were photographed, and photographed images were evaluated by the use of an image quality figure (IQF)[11)].

2. Materials and Methods

2.1. Equipment

An ISS-FPD system (CALNEO MT, FUJIFILM Corporation, Tokyo, Japan) and a conventional CR system (FCR9502HQ, FUJIFILM Corporation, Tokyo, Japan) were used. Both of the systems are of the lying-position X-ray photographing table type, and are each equipped with an anti-scatter grid. The details of the digital imaging systems are shown in Table 1. For the FPD system, an X-ray generator (UD150B-40, Shimadzu, Kyoto, Japan) and an X-ray tube (P364DK-85, Shimadzu, Kyoto, Japan) were used. For the CR system, an X-ray generator (KXO-80G, Toshiba, Tochigi, Japan) and an X-ray tube (DRA3724HD, Toshiba, Tochigi, Japan) were used. Experiments were conducted at a source-image receptor distance (SID) within the range of 150–155 cm.

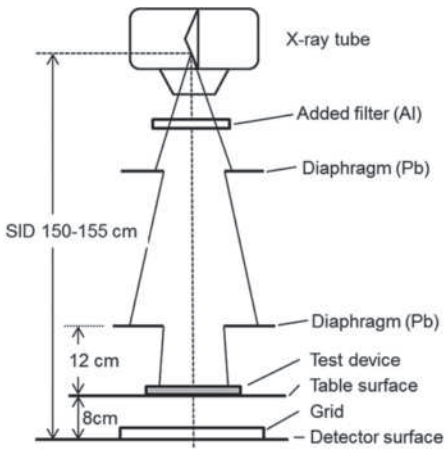

Fig. 1. Geometry for exposing the digital X-ray imaging device.

2.2. Image quality

Experimental arrangement conformed to IEC6 2220-1[10)] (Figure 1). As the radiation quality of X-ray beams for image quality evaluation, an RQA5 [additional filtration 21.0 mm A1, half-value layer (HVL) 7.1mm Al] and an RQA7 (additional filtration 30.0 mm A1, HVL 9.1 mm A1) were used[9, 10)]. A reference incident surface dose was set to 8.76μGy (1 mR), and irradiation was performed within the range of $1/16^{th}$ to 8 times the reference dose, according to need. For measurements of incident doses and HVLs, a semiconductor detector (RaySafe Xi,

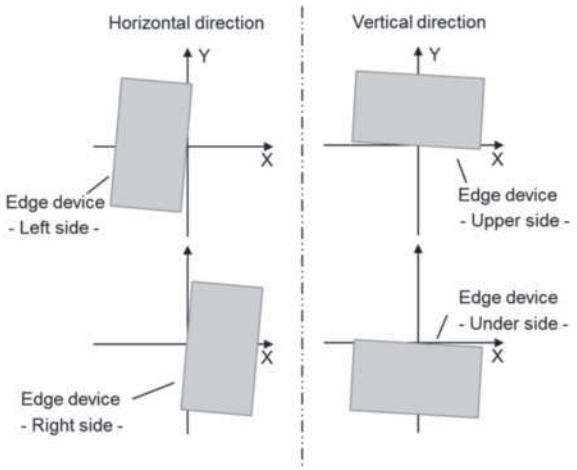

Fig. 2. Lay of the edge device placement

Uniforce RaySafe, Billdal, Sweden) was used.

Digital characteristic curves, pre-sampled MTFs, NNPSs, and DQEs of the ISS-FPD system and the CR system, each equipped with an anti-scatter moving grid, were measured and compared. For concrete details of the measurements, we referred to, "Image quality measurement of digital radiography, Ohm-sha, Tokyo, Japan,"[12] conforming to IEC 62220-1. Regarding acquisition of digital image data, read was carried out with the fixed sensitivity ("S" value) of 200 and the latitude ("L" value) of 4[13] in the test mode of both the ISS-FPD and the CR systems.

Digital characteristic curves were obtained from the average value of 3 independent measurements by the time-scale method[14]. The digital characteristic curves were employed for linearization of the pre-sampled MTF and NNPS measurements. Therefore, doses for preparation of digital characteristic curves were within the range of 1/16th to 8 times the reference dose. Measurements of pre-sampled MTFs were carried out by the edge method[10, 12]. Pre-sampled MTFs were derived from the average value of three independent measurements. It is known that a pre-sampled MTF of the CR system depends on the arrangement direction of the edge[15, 16]. Therefore, pre-sampled MTFs in 4 total directions were found with the edge displayed as shown in Figure 2. The edge method is strongly influenced by noise[17]. In order to reduce this influence, a method utilizing a bin was used for preparation of a synthetic edge spread function (ESF)[12, 18]. For a line spread function (LSF) found from the ESF, a method in which a skirt part is not extrapolated was used[12]. NNPSs were selected from images evenly irradiated under various exposure conditions. Two-dimensional trend processing was executed after a pixel value was linearized by a digital characteristic curve, and then a two-dimensional NNPS

Table 2. Detective quantum efficiency (DQE) ratio of computed radiography (CR) to irradiation side sampling flat-panel device (ISS-FPD)

Spatial frequency	Vertical		Horizontal	
	RQA5	RQA7	RQA5	RQA7
1 cycles/mm	0.63	0.73	0.60	0.69
2 cycles/mm	0.44	0.53	0.37	0.38
3 cycles/mm	0.30	0.47	0.24	0.33
Average	0.46	0.55	0.40	0.47

was calculated using a 2D fast Fourier transform. One-dimensional NNPSs in the horizontal direction and the vertical direction were calculated from two-dimensional NNPS data[12]. With measured average pre-sampled MTFs and an NNPS at the reference dose used, the DQEs in both the vertical direction and the horizontal direction were found by the following expression:

$$\mathrm{DQE}(u) = \frac{\text{pre–sampled MTF}^2\,(u)}{\mathrm{NNPS}(u) \cdot q}$$

where u is a special frequency (cycles/mm), and q is the number of incident photons. The number of photons was 30174[1/(mm^2· μGy)] at RQA5 and 32362[1/(mm^2· μGy)] at RQA7[10]. The total number of incident photons was found by multiplying a measured incident dose by the number of photons at RQA5 and the number of photons at RQA7, and then, correction of the distance and correction using a table-absorbing material were performed[12]. Nyquist frequencies of the ISS-FPD system and the CR system were 3.3 and 5.0 cycles/mm, respectively.

2.3. Visual evaluation

A convex Burger phantom was arranged at a position near the test device in Figure 1, and photographed at the reference dose and 1/16th- to double-doses. Conditions of the radiation quality and acquisition of digital image data were the same as mentioned in Section 2.1 for both the ISS-FPD and the CR systems. Next, in order to add a scatter, a Mix-Dp (5-cm) phantom was added between the Burger phantom and the table surface and the Burger phantoms were photographed under the same conditions. For visual evaluation, observation was performed by 5 observers with the use of a 5-mega-pixel high-definition monitor, and IQFs were calculated from the following expression[11]:

$$\mathrm{IQF} = \sum_{i=1}^{n} (Di^{*}hi)$$

where Di is the size (mm) of the diameter of each Burger phantom, and hi is the identifiable minimum height (mm).

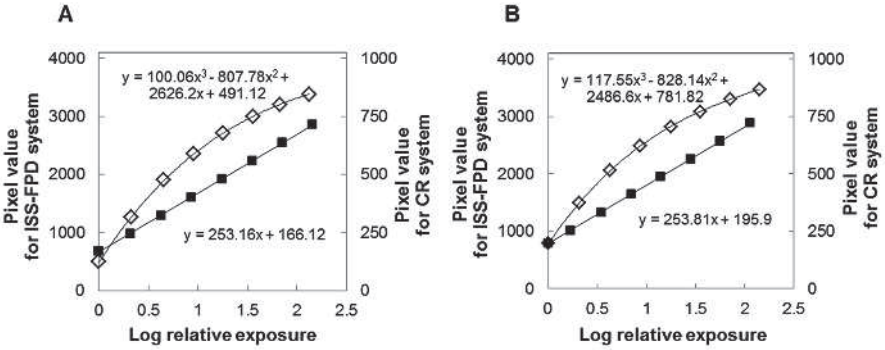

Fig. 3. Digital characteristic curves for the ISS-FPD and CR systems in RQA5 and RQA7: A, RQA5; B, RQA7; ◇, ISS-FPD system; ■, CR system

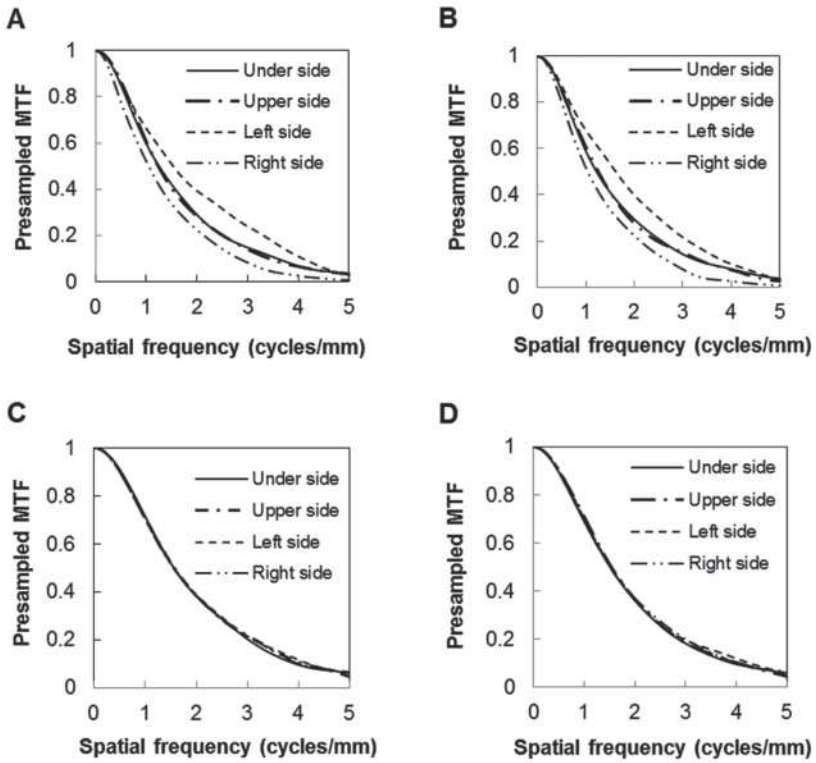

Fig. 4. Comparison of pre-sampled MTFs for the ISS-FPD and CR systems in the lay of edge device placement: A, RQA5 CR; B, RQA7 CR; C, RQA5 ISS-FPD; D, RQA7 ISS-FPD.

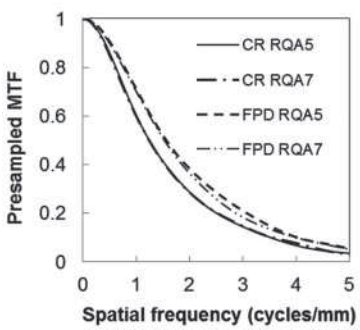

Fig. 5. Comparison of pre-sampled MTFs for the ISS-FPD and CR systems in the vertical direction.

3. Results

Digital characteristic curves at RQA5 and RQA7 are shown in Figure 3. As for radiation qualities obtained from the CR system, pixel values were proportional to the logarithmic values of doses. On the other hand, in the case of the ISS-FPD system, the relationship between the logarithmic values of doses and pixel values was a cubic function.

Pre-sampled MTFs in the edge arrangement direction at each radiation quality are shown in Figure 4. In the case of the CR system at both RQA5 and RQA7, there was no difference in pre-sampled MTFs in the arrangement

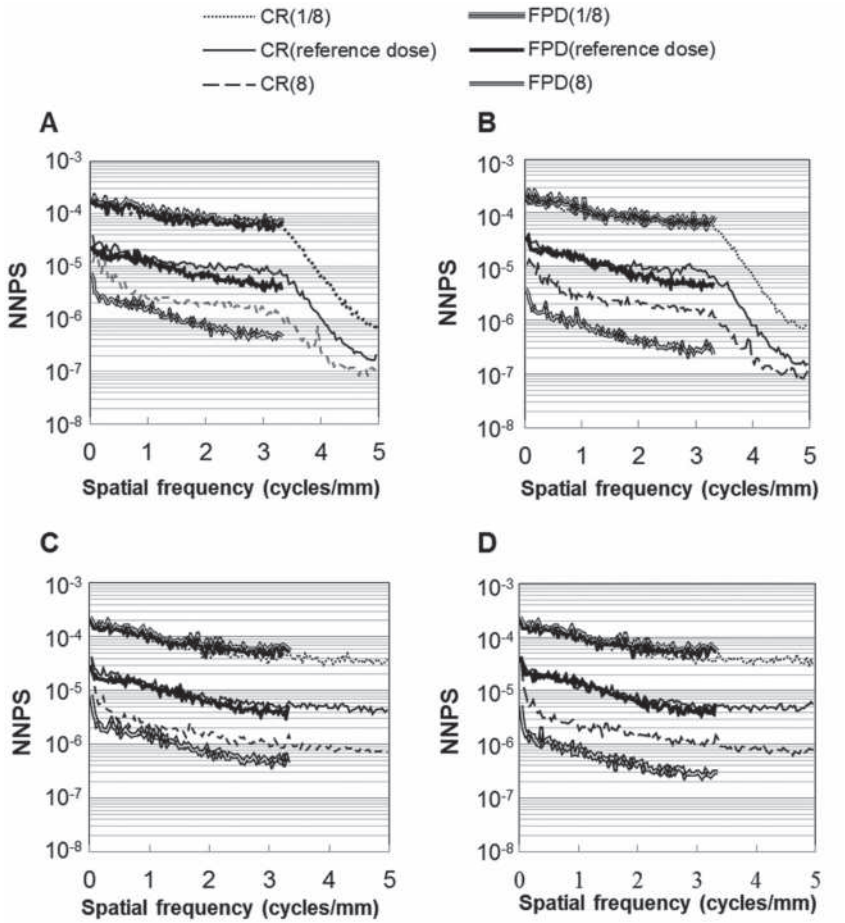

Fig. 6. NNPSs for the ISS-FPD and CR systems in the vertical and horizontal directions under various exposure conditions: A, RQA5, horizontal direction; B, RQA7, horizontal direction; C, RQA5, vertical direction; D, RQA7, vertical direction.

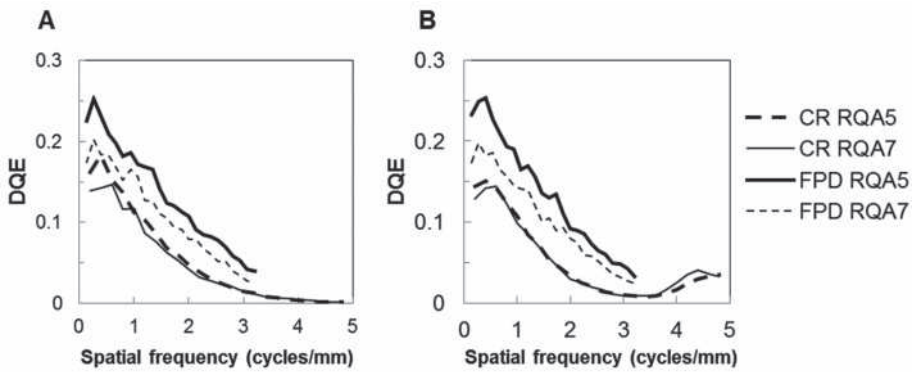

Fig. 7. DQEs for the ISS-FPD and CR systems in the vertical and horizontal directions under the same exposure conditions: A, vertical direction; B, horizontal direction.

direction of the upper side versus the underside (ie, in the vertical direction), but there was a difference in pre-sampled MTFs between the left side and the right side (ie, in the horizontal direction). In the case of the ISS-FPD system, similar values were obtained in all arrangement directions. Pre-sampled MTFs of the CR system and the ISS-FPD system in the vertical direction are shown in Figure 5. In comparison between the ISS-FPD and the CR systems, it is understood that the ISS-FPD system has higher resolution. Results showed that the pre-

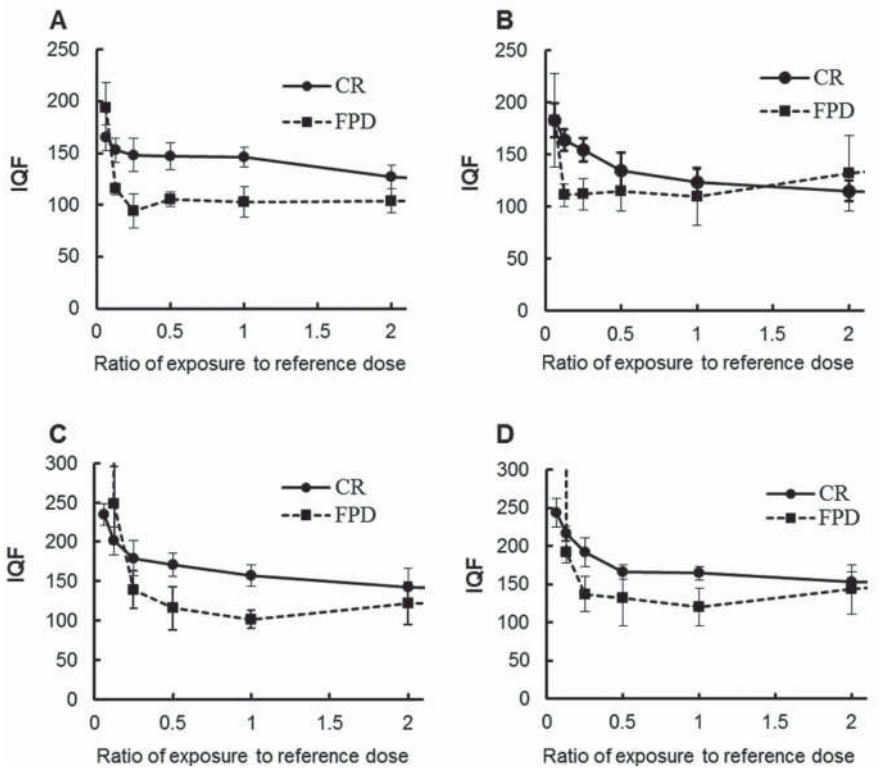

Fig. 8. IQFs for the ISS-FPD and CR systems in RQA5 and RQA7 conditions with and without phantom: A, no RQA5-added phantom; B, no RQA7-added phantom; C, RQA5-added phantom; D, RQA7-added phantom; Data are expressed as mean ± SD of 5 observers.

sampled MTFs of the ISS-FPD system were higher than those of the CR system by approximately 17% in a spatial frequency of 1 cycle/mm, and by approximately 25% in 2 cycles/mm.

NNPSs at each radiation quality, which were obtained at different doses in each direction, are shown in Figure 6. In all cases, the higher an incident dose was, the smaller the NNPS was. The ISS-FPD system showed NNPSs lower than those of the CR system at a dose as high as 8 times the reference dose, but the NNPS of the ISS-FPD and the CR systems were almost the same at the reference dose and low doses. Furthermore, lowering of the NNPSs in a high-frequency region was seen in the horizontal direction of the CR system, and the peak considered to be caused by a moving grid was seen near 4 cycles/mm at a high dose.

DQEs at each radiation quality and in each modality are shown in Figure 7. In all cases, the higher a special frequency was, the lower a DQE value was. We observed that the DQEs of the ISS-FPD system were higher than those of the CR system. At 1 cycle/mm in the vertical direction, DQE values of the CR system were 0.12 at RQA5 and 0.12 at RQA7, and those of the ISS-FPD system were 0.18 at RQA5 and 0.16 at RQA7. DQE ratios of the CR system to the ISS-FPD system in each frequency are shown in Table 2. The CR system showed an average value accounting for approximately 50% of that of the ISS-FPD system.

Results of the visual evaluation are shown in Figure 8. When the reference dose was irradiated under the condition of no RQA5-added phantom (Fig. 8A), IQFs of the ISS-FPD system were significantly lower ($P < 0.01$) in comparison with those of the CR system. Also, in reference dose irradiation with an RQA5-added phantom and reference dose irradiation with an RQA7-added phantom (Fig. 8C, D), the IQFs of the ISS-FPD system were significantly lower than those of the CR system ($P < 0.01$). In reference dose irradiation without an RQA7-added phantom (Fig. 8B), there was no difference between the IQFs of the ISS-FPD system and those of the CR system. Then, doses of the ISS-FPD system were examined at the same IQF value and at the same time of reference dose irradiation of the CR system, and the following values were obtained: in the case without an RQA5-added phantom, 0.10; with an RQA5-added phantom, 0.23; without an RQA7 phantom, 0.11; and with an RQA7-added phantom, 0.19. Furthermore, since the IQF variation of the CR system was great, an average and a standard deviation of an IQF at each dose were calculated. As a result, at the reference dose, a half-dose,

and a quarter-dose, values of 148 ± 18, 155 ± 17 and 169 ± 21 were obtained for the CR system respectively, and 109 ± 8, 117 ± 11 and 121 ± 21 were obtained for the ISS-FPD system respectively, suggesting that the IQFs of the CR system were larger than those of the ISS-FPD system and also varied widely.

4. Discussion

When the image quality of a table-integrated ISS-FPD or CR system is measured, it is difficult to remove the grid. Therefore, we measured image qualities with the grid installed for the ISS-FPD and the CR systems and a significant difference was found. In comparing the DQEs, it was suggested that, in the case of the ISS-FPD system, the reduction of radiation exposure of approximately 50% (Table 2) of that of the CR system is possible. Tanaka *et al* also reported that a reduction of radiation exposure by 50% is possible in chest radiography with the use of an ISS-FPD[8]. The DQE cannot be related to the presence or absence of a grid theoretically, but since the reduction of the number of incident photons at a grid cannot be measured, correction for the grid was not made. It is therefore possible that the DQEs were calculated to be lower than the actual value. However, it is considered that the calculated DQEs can be compared with the use of a ratio of a DQE to another modality similarly calculated. As doses of the ISS-FPD system at which an IQF becomes the same as that of the reference dose of the CR system are 0.1 to 0.23 times that of the reference dose in visual evaluation, it is considered that a reduction of radiation exposure by approximately 80-90% is possible.

As for digital characteristic curves (Fig. 3), while the CR system showed a straight line, the ISS-FPD system showed a curved line. The purpose of these digital characteristic curves is for linearization of pre-sampled MTF and NNPS measurement. Therefore, digital characteristic curves of the ISS-FPD system were used without being processed.

There was a large difference in pre-sampled MTFs between the left side and the right side of the CR system. A large difference was found in the horizontal direction, which was the main scanning direction of the data-collecting mechanism[12]. We considered the possibility that the pre-sampled MTFs in the main scanning direction were influenced by a low-pass filter for aliasing error reduction, and thereby the difference was produced[19]. A low-pass filter works only in the main scanning direction, and the pre-sampled MTFS were not influenced by low-pass filter processing in the vertical direction (the sub-scanning direction). Pre-sampled MTFs of the ISS-FPD system showed values approximately 20% higher than those of the CR system. We thus confirmed that the ISS method is hardly affected by light diffusion in comparison with a conventional PSS method and has excellent resolution[7].

In comparison with NNPSs in the horizontal direction and the vertical direction of the CR system, higher frequency portions in the horizontal direction showed lower values than those in the vertical direction (Fig. 6). This is also considered to be caused by the influence of the low-pass filter in the main scanning direction[12]. A low-pass filter attenuates components with a Nyquist frequency or higher and reduces aliasing errors.

5. Conclusion

As for resolution, the ISS-FPD system was excellent, whereas for noise characteristics, the CR and the ISS-FPD systems were at the same level. Regarding DQEs, because the ISS-FPD system showed higher values than those of the CR system, it can be said that the ISS-FPD system is excellent in image quality and can reduce the incident surface dose. Since visual evaluation was also better in the case of the ISS-FPD system than in the CR system, the possibility that the ISS-FPD system can reduce radiation exposure of a patient was also suggested.

Acknowledgements

I am deeply grateful to the students of The School of Health Sciences, Medical Department at Hirosaki University, Mr. Keisuke Araki, Ms. Siori Sasaki, Mr. Shungo Takahasi and Ms. Yurie Nakagawara, who cooperated with me in this scientific study.

References

1. Sonoda M Takano M Miyahara J and Kato H (1983) Computed radiography utilizing scanning laser stimulated luminescence. Radiology 148:833–838.
2. Kishimoto Kenji, et al. (2011) Study of appropriate dosing in consideration of image quality and patient dose on the digital radiography. Jpn J Radiological Technology 67:1381–1397. (in Japanese)
3. Bacher K, et al. (2003) Dose reduction in patients undergoing chest imaging: digital amorphous silicon flat-panel detector radiography versus conventional film-screen radiography and phosphor-based computed radiography. Am J Roentgenol 181:923–929.
4. Schaefer-Prokop C, et al. (2008) Digital chest radiography: an update on modern technology, dose containment and control of image quality. Eur Radiol 18:1818–1830.
5. Yokoi T Takata T and Ichikawa K (2011) Investigation of image quality identification utilizing physical image quality measurement in direct- and indirect-type of flat panel detectors and computed radiography. Jpn J Radiological Technology 67:1415–1424. (in Japanese)
6. Tsukamoto A, et al. (2012) Summary of results of the patient exposures in diagnostic radiography in (2011) questionnaire - focus on radiographic conditions -. Jpn J Radiological Technology 68: 1261–1268. (in Japanese)
7. Sato K, et al. (2010) Development of "CALNEO", an indirect-

conversion digital radiography system with high-conversion efficiency. Fujifilm Res 55:10–13. (in Japanese)

8. Tanaka N, et al. (2013) Basic imaging properties of an indirect flat-panel detector system employing irradiation side sampling (ISS) technology for chest radiography: comparison with a computed radiographic system. Radiol Phys Technol 6:162–169.
9. IEC 61267 Ed. 1.0 (1994) Medical diagnostic X-ray equipment—radiation conditions for use in the determination of characteristics. The International Electrotechnical Commission.
10. IEC 62220-1 Ed. 1.0 (2003) Medical electrical equipment—characteristics of digital X-ray imaging devices—part 1: determination of the detective quantum efficiency. The International Electrotechnical Commission.
11. Mochizuki Y Abe S and Yamaguchi K (2009) Estimation of appropriate dose for computed radiography by the threshold value of the image quality figure. Jpn J Radiological Technology 65: 430-437. (in Japanese)
12. Ichikawa and K Ishida T (2011) Image quality measurement of digital radiography. pp.109–224. Ohm-Sha, Tokyo.
13. Kawaharada M Ishida T Okura Y and Kawashita I (2010) Relationship between image quality and signal detectability in CR and FPD Systems. Jpn J Radiological Technology 66:1449–1456. (in Japanese)
14. Kanai K, et al. (1988) Comparison of measurement methods of characteristic curves for digital subtraction angiography (DSA) systems. Jpn J Radiological Technology 44:1492–1496. (in Japanese)
15. Fetterly KA Hangiandreou NJ Schueler BA and Ritenour ER (2002) Measurement of the pre-sampled two-dimensional modulation transfer function of digital imaging systems. Med Phys 29:913–921.
16. Fetterly KA and Schueler BA (2003) Performance evaluation of a "dual-side read" dedicated mammography computed radiography system. Med Phys 30:1843–1854.
17. Samei E Ranger NT Dobbins JT Chen Y (2006) Intercomparison of methods for image quality characterization. I. Modulation transfer function. Med Phys 33:1454–1465.
18. Higashide R Ichikawa K Kunitomo H and Sawada M (2008) Proposal and verification of pre-sampled MTF measurement by the simple analysis method using the edge method. Jpn J Radiological Technology 64:417–425. (in Japanese)
19. Mochizuki Y Kasahara R Ueda D and Takeda M (2013) Measurement of pre-sampled MTFs with computed radiography (CR) by contrast method using smoothed square-wave. Jpn Association Radiological Technologists 60:35–39. (in Japanese)